

1  
2  
3  
4  
5  
6  
7  
8  
9  
10  
11  
12  
13  
14  
15  
16  
17  
18  
19

**Bacterial biodiversity drives the evolution of CRISPR-based phage resistance**

Ellinor O Alseth<sup>1\*</sup>, Elizabeth Pursey<sup>1</sup>, Adela M Luján<sup>2</sup>, Isobel McLeod<sup>1</sup>, Clare Rollie<sup>1</sup>, Edze R Westra<sup>1\*</sup>

*<sup>1</sup>Environment and Sustainability Institute, Biosciences, University of Exeter, Cornwall Campus, Penryn, Cornwall TR10 9FE, United Kingdom*

*<sup>2</sup>IRNASUS, CONICET, Facultad de Ciencias Químicas, Universidad Católica de Córdoba, Avda. Armada Argentina 3555, X5016DHK, Córdoba, Argentina*

*\*Correspondence: E.R.Westra@exeter.ac.uk, eao210@exeter.ac.uk*

Keywords: CRISPR-Cas; *Pseudomonas aeruginosa*; cystic fibrosis; fitness trade-offs; evolution of virulence; biodiversity; phage

20 **Approximately half of all bacterial species encode CRISPR-Cas adaptive immune**  
21 **systems<sup>1</sup>, which provide immunological memory by inserting short DNA sequences from**  
22 **phage and other parasitic DNA elements into CRISPR loci on the host genome<sup>2</sup>. Whereas**  
23 **CRISPR loci evolve rapidly in natural environments<sup>3,4</sup>, bacterial species typically evolve**  
24 **phage resistance by the mutation or loss of phage receptors under laboratory**  
25 **conditions<sup>5,6</sup>. Here, we report how this discrepancy may in part be explained by**  
26 **differences in the biotic complexity of *in vitro* and natural environments<sup>7,8</sup>. Specifically,**  
27 **using the opportunistic pathogen *Pseudomonas aeruginosa* and its phage DMS3vir, we**  
28 **show that coexistence with other human pathogens amplifies the fitness trade-offs**  
29 **associated with phage receptor mutation, and therefore tips the balance in favour of**  
30 **CRISPR-based resistance evolution. We also demonstrate that this has important knock-**  
31 **on effects for *P. aeruginosa* virulence, which became attenuated only if the bacteria**  
32 **evolved surface-based resistance. Our data reveal that the biotic complexity of microbial**  
33 **communities in natural environments is an important driver of the evolution of CRISPR-**  
34 **Cas adaptive immunity, with key implications for bacterial fitness and virulence.**

35

36 *Pseudomonas aeruginosa* is a widespread opportunistic pathogen that thrives in a range of  
37 different environments, including hospitals, where it is a common source of nosocomial  
38 infections. In particular, it frequently colonises the lungs of cystic fibrosis patients, in whom it  
39 is the leading cause of morbidity and mortality<sup>9</sup>. In part fuelled by a renewed interest in the  
40 therapeutic use of bacteriophages as antimicrobials (phage therapy)<sup>10,11</sup>, many studies have  
41 examined if and how *P. aeruginosa* evolves resistance to phage (reviewed in ref. 12). The  
42 clinical isolate *P. aeruginosa* strain PA14 has been reported to predominantly evolve resistance  
43 against its phage DMS3vir by the modification or complete loss of the phage receptor (Type  
44 IV pilus) when grown in nutrient-rich medium<sup>5</sup>, despite carrying an active CRISPR-Cas  
45 adaptive immune system (Clustered Regularly Interspaced Short Palindromic Repeats;  
46 CRISPR-associated). Conversely, under nutrient-limited conditions, the same strain relies on  
47 CRISPR-Cas to acquire phage resistance<sup>5</sup>. These differences are due to higher phage densities  
48 during infections in nutrient-rich compared to nutrient-limited conditions, which in turn  
49 determines whether surface-based resistance (with a fixed cost of resistance) or CRISPR-based  
50 resistance (infection-induced cost) is favoured by natural selection<sup>5,13</sup>. While these  
51 observations suggest abiotic factors are critical determinants of the evolution of phage  
52 resistance strategies, the role of biotic factors has remained unclear, even though *P. aeruginosa*  
53 commonly co-exists with a range of other bacterial species in both natural and clinical

54 settings<sup>14,15</sup>. We hypothesised that the presence of a bacterial community could drive increased  
55 levels of CRISPR-based resistance evolution for mainly two reasons. Firstly, reduced *P.*  
56 *aeruginosa* densities in the presence of competitors may limit phage amplification, favouring  
57 CRISPR-based resistance<sup>5</sup>. Secondly, pleiotropic costs associated with phage receptor  
58 mutation may be amplified during interspecific competition.

59 To explore these hypotheses, we co-cultured *P. aeruginosa* PA14 with three other  
60 clinically relevant opportunistic pathogens that are known to co-infect with *P. aeruginosa*,  
61 namely *Staphylococcus aureus*, *Burkholderia cenocepacia*, and *Acinetobacter baumannii*<sup>14-17</sup>,  
62 none of which can be infected by or interact with phage DMS3vir (Extended Data Fig. 1). We  
63 applied a “mark-recapture” approach using a *P. aeruginosa* PA14 mutant carrying  
64 streptomycin resistance in order to monitor the bacterial population dynamics and phage  
65 resistance evolution in the focal subpopulation at 3 days post infection (d.p.i.). This revealed  
66 that in nutrient-rich Lysogeny Broth, PA14 evolved significantly higher levels of CRISPR-  
67 based resistance following infection with 10<sup>6</sup> plaque forming units (p.f.u.) of phage DMS3vir  
68 when co-cultured with other bacterial species compared to when grown in isolation or co-  
69 cultured with an isogenic surface mutant (Fig. 1a). Additionally, we found that these effects  
70 were dependent on the identity of the species that were present in the mixed culture, with the  
71 strongest effects being observed in the presence of *A. baumannii* or a mix of the three bacterial  
72 species, and an absence of any effect when PA14 was co-cultured with an isogenic surface  
73 mutant that lacked the phage receptor (Fig. 1a, Deviance test: Relationship between community  
74 composition and CRISPR; Residual deviance(30, n = 36) = 1.81, p = 2.2 x 10<sup>-16</sup>; Tukey  
75 contrasts: Monoculture v Mixed; z = -5.99, p = 3.02 x 10<sup>-8</sup>; Monoculture v *A. baumannii*; z =  
76 -4.33, p = 0.00023; Monoculture v *B. cenocepacia*; z = -3.76, p = 0.0026; Monoculture v *S.*  
77 *aureus*; z = -2.38, p = 0.26; Monoculture v surface mutant; z = 2.26, p = 0.35). Interestingly,  
78 *P. aeruginosa* densities were strongly reduced in the presence of *A. baumannii*, *B. cenocepacia*  
79 and the mixed community, while on the other hand it dominated the community during  
80 competition with *S. aureus* despite the presence of phage DMS3vir (Fig. 1b), suggesting a  
81 positive relationship between the strength of interspecific competition and the levels of  
82 CRISPR-based resistance evolution.

83 Next, to explore the clinical relevance of this observation, we performed a similar  
84 experiment in artificial sputum medium (ASM), which is a nutrient rich medium that mimics  
85 the abiotic environment of sputum from cystic fibrosis patients<sup>18</sup>. This revealed a similar  
86 pattern as that observed in Lysogeny Broth, with *A. baumannii* and the community as a whole  
87 resulting in a drastic increase in CRISPR-based resistance evolution (Extended Data Fig. 2).

88 To further explore the generality of these findings, we also manipulated the microbial  
89 community composition by varying the proportion of *P. aeruginosa* versus the other pathogens.  
90 This revealed that increased CRISPR-based resistance evolution occurred across a wide range  
91 of microbial community compositions, with a maximum effect size when *P. aeruginosa* made  
92 up 50% of the initial mixture (Extended Data Fig. 3). An exception to this trend was when the  
93 *P. aeruginosa* subpopulation made up only 1% of the total community; in this case sensitive  
94 bacteria persisted alongside resistant bacteria because of the reduced size of the phage epidemic  
95 and hence relaxed selection for resistance (Extended Data Fig. 3). Collectively, these data  
96 suggest that greater levels of interspecific competition contribute to the evolution of CRISPR-  
97 based resistance.

98 We hypothesised that reduced *P. aeruginosa* population sizes in the presence of  
99 competitors might explain the increased evolution of CRISPR-based resistance, as this leads  
100 to smaller phage epidemics, which is known to favour CRISPR over surface-based resistance<sup>5</sup>.  
101 However, variation in the force of infection did not seem to play a strong role in the observed  
102 effects, since even though phage epidemic sizes varied depending on the microbial community  
103 composition (Extended Data Fig. 4), this did not correlate with the levels of evolved CRISPR-  
104 resistance (Extended Data Fig. 5). Moreover, when manipulating the DMS3vir starting phage  
105 titres, we observed no differences in the levels of evolved CRISPR-based resistance when *P.*  
106 *aeruginosa* was co-cultured in the presence of the microbial community (Extended Data Fig.  
107 6). An alternative explanation for the observed effects may therefore be that the fitness cost of  
108 surface-based resistance is amplified in the presence of other bacterial species, for example due  
109 to cell surface molecules playing a part in interspecific competition<sup>19</sup>, which again would result  
110 in stronger selection towards bacteria with CRISPR-based resistance. To test this hypothesis,  
111 we competed the two phage resistant phenotypes (i.e. CRISPR-resistant and surface mutant) in  
112 the presence or absence of the microbial community, and across a range of phage titres. In the  
113 absence of the microbial community and phage, CRISPR-resistant bacteria showed a small  
114 fitness advantage over bacteria with surface-based resistance, but this advantage disappeared  
115 when phage was added and as titres increased (Fig. 2a, and ref. 5). In the presence of the  
116 biodiverse microbial community however, the relative fitness of bacteria with CRISPR-based  
117 resistance was consistently higher, demonstrating that mutation of the Type IV pilus is more  
118 costly when bacteria compete with other bacterial species (Fig. 2a, Linear model: Effect of  
119 community absence;  $t = -5.54$ ,  $p = 1.49 \times 10^{-7}$ ; Effect of increasing phage titre;  $t = -2.41$ ,  $p =$   
120  $0.017$ ; Overall model fit; Adjusted  $R^2 = 0.41$ ,  $F_{4,139} = 25.48$ ,  $p = 7.65 \times 10^{-16}$ ). The increased  
121 fitness trade-off associated with surface-based resistance was also observed when the CRISPR-

122 and surface-resistant phenotypes competed in the presence of only a single additional species  
123 (Fig. 2b, Two-way ANOVA with Tukey contrasts: Overall difference in fitness;  $F_{4,2} = 8.151$  p  
124  $= 6.31 \times 10^{-6}$ ; Monoculture v Mixed;  $p = 0.011$ ; Monoculture v *A. baumannii*;  $p = 0.016$ ;  
125 Monoculture v *B. cenocepacia*;  $p = 0.022$ ), with the exception of *S. aureus* (Fig. 2d.  
126 Monoculture v *S. aureus*;  $p = 0.80$ ), concordant with this species being the weakest competitor  
127 and inducing the lowest levels of CRISPR-based resistance (Fig. 1). These fitness trade-offs  
128 therefore explain why *P. aeruginosa* evolved greater levels of CRISPR-based resistance in the  
129 presence of the other pathogens, and why this varied depending on the competing species (Fig.  
130 1).

131 Evolution of phage resistance by bacterial pathogens is often associated with virulence  
132 trade-offs when surface structures are modified<sup>20</sup>, whereas similar trade-offs have not yet been  
133 reported in the literature for CRISPR-based resistance. We therefore hypothesised that the  
134 community context in which phage resistance evolves may have important knock-on effects  
135 for *P. aeruginosa* virulence. To test this, we used a *Galleria mellonella* infection model, which  
136 is commonly used to evaluate virulence of human pathogens<sup>21,22</sup>. We compared *in vivo*  
137 virulence of *P. aeruginosa* clones that evolved phage resistance against phage DMS3vir in  
138 different community contexts by injecting larvae with a mixture of clones that had evolved  
139 phage-resistance in either the presence or absence of the mixed bacterial community (Extended  
140 Data. Fig. 3c). Taking time to death as a proxy for virulence, we found that the evolution of  
141 phage resistance in the presence of a microbial community was associated with greater levels  
142 of *P. aeruginosa* virulence compared to when phage-resistance evolved in monoculture, and  
143 remained similar to that of the ancestral PA14 strain (Fig. 3a, Cox proportional hazards model  
144 with Tukey contrasts: Community present v absent;  $z = 5.85$ ,  $p = 1 \times 10^{-4}$ ; ancestral PA14 v  
145 community absent;  $z = 4.42$ ,  $p = 1 \times 10^{-4}$ ; ancestral PA14 v community present;  $z = -1.30$ ,  $p =$   
146  $0.38$ . Overall model fit;  $LRT_3 = 51.03$ ,  $n = 376$ ,  $p = 5 \times 10^{-11}$ ). These data, in combination with  
147 the fact that the Type IV pilus is a well-known virulence factor<sup>23</sup>, are consistent with the notion  
148 that the mechanism by which bacteria evolve phage resistance has important implications for  
149 bacterial virulence. To more directly test this, we next infected larvae with each individual *P.*  
150 *aeruginosa* clone for which we had previously determined the mechanism underlying evolved  
151 phage resistance (Extended Data Fig. 3c), again using time to death as a measure of virulence.  
152 This showed that bacterial clones with surface-based resistance - unlike those with CRISPR-  
153 based resistance - both had drastically reduced swarming motility (as expected with mutations  
154 in the Type IV pilus<sup>23</sup>) (Fig. 3b, One-way ANOVA with Tukey contrasts: Overall effect;  $F_{2,977}$   
155  $= 472.5$ ,  $p = 2.2 \times 10^{-16}$ ; Sensitive v CRISPR;  $p = 0.87$ ; CRISPR v Surface mutant ;  $p = 1 \times 10^{-$

156 <sup>5</sup>) and impaired virulence compared to phage sensitive bacteria (Fig. 3c, Cox proportional  
157 hazards model with Tukey contrasts: Surface mutant v CRISPR;  $z = -2.37$ ,  $p = 0.045$ ; Sensitive  
158 v CRISPR;  $z = 2.10$ ,  $p = 0.10$ ; Surface mutant v Sensitive;  $z = -4.23$ ,  $p = 1 \times 10^{-3}$ . Overall  
159 model fit;  $LRT_3 = 48.66$ ,  $n = 981$ ,  $p = 2 \times 10^{-10}$ ). Similar virulence trade-offs were also observed  
160 when larvae were injected with *P. aeruginosa* PA14 clones that had evolved surface-based  
161 resistance against phage LMA2, which uses LPS (lipopolysaccharide) as a receptor (Extended  
162 Data Fig. 7), in agreement with the idea that phage receptor mutations are commonly associated  
163 with *in vivo* virulence trade-offs.

164 Collectively, our data show that the evolutionary outcome of bacteria-phage  
165 interactions can be fundamentally altered by the microbial community context. While  
166 traditionally studied in isolation, these interactions are usually embedded in complex biotic  
167 networks of multiple species, and it is becoming increasingly clear that this can have key  
168 implications for the evolutionary epidemiology of infectious disease<sup>24–28</sup>. The work presented  
169 here reveals that the community context can also shape the evolution of different host resistance  
170 strategies. Specifically, we find that the interspecific interactions between four bacterial species  
171 in a synthetic microbial community can have a large impact on the evolution of phage  
172 resistance mechanisms by amplifying the constitutive fitness cost of surface-based resistance<sup>5</sup>.  
173 The finding that biotic complexity matters complements previous work on the effect of abiotic  
174 variables and the force of infection on phage resistance evolution<sup>5</sup>. The data presented here  
175 suggests that the impact of biotic complexity on the evolution of CRISPR-based resistance is  
176 stronger than that of variation in phage abundance, which is consistent with the observation  
177 that in the presence of the polymicrobial community, bacteria with CRISPR-based resistance  
178 outcompeted bacteria with surface-based resistance at all phage titres (Fig. 2). The amplified  
179 fitness cost of surface mutation also suggest that the type Type IV pilus plays an important role  
180 in interspecific competition. While future work will be critical to understand the detailed  
181 molecular mechanism that underpins these effects, and to further generalise the findings  
182 described here to other bacterial species and strains, we speculate that the way in which the  
183 microbial community composition drives the evolution of phage resistance strategies may be  
184 important in the context of phage therapy. Primarily, the absence of detectable trade-offs  
185 between CRISPR-based resistance and virulence, as opposed to when bacteria evolve surface-  
186 based resistance, suggests that evolution of CRISPR-based resistance can ultimately influence  
187 the severity of disease. Moreover, evolution of CRISPR-based resistance can drive more rapid  
188 phage extinction<sup>29</sup>, and may in a multi-phage environment result in altered patterns of cross-  
189 resistance evolution compared to surface-based resistance<sup>30</sup>. The identification of the drivers

190 and consequences of CRISPR-resistance evolution might help to improve our ability to predict  
191 and manipulate the outcome of bacteria-phage interactions in both natural and clinical settings.

192

193 1. Grissa, I., Vergnaud, G. & Pourcel, C. CRISPRcompar: a website to compare clustered  
194 regularly interspaced short palindromic repeats. *Nucleic Acids Res.* **36**, 52–57 (2008).

195 2. Barrangou, R. *et al.* CRISPR provides acquired resistance against viruses in prokaryotes.  
196 *Science* **315**, 1709–12 (2007).

197 3. Andersson, A. F. & Banfield, J. F. Virus population dynamics and acquired virus  
198 resistance in natural microbial communities. *Science* **320**, 1047–1050 (2008).

199 4. Laanto, E., Hoikkala, V., Ravantti, J. & Sundberg, L. R. Long-term genomic coevolution  
200 of host-parasite interaction in the natural environment. *Nat. Commun.* **8** (2017).

201 5. Westra, E. R. *et al.* Parasite exposure drives selective evolution of constitutive versus  
202 inducible defense. *Curr. Biol.* **25**, 1043–1049 (2015).

203 6. van Houte, S., Buckling, A. & Westra, E. R. Evolutionary ecology of prokaryotic  
204 immune mechanisms. *Microbiol. Mol. Biol. Rev.* **80**, 745–763 (2016).

205 7. Hibbing, M. E., Fuqua, C., Parsek, M. R. & Peterson, S. B. Bacterial competition:  
206 surviving and thriving in the microbial jungle. *Nat. Rev. Microbiol.* **8**, 15–25 (2010).

207 8. O’Toole, G. A. Cystic fibrosis airway microbiome: overturning the old, opening the way  
208 for the new. *J. Bacteriol.* **200**, 1–8 (2017).

209 9. Folkesson, A. *et al.* Adaptation of *Pseudomonas aeruginosa* to the cystic fibrosis  
210 airway: an evolutionary perspective. *Nat. Rev. Microbiol.* **10**, 841–51 (2012).

211 10. Roach, D. R. & Debarbieux, L. Phage therapy: awakening a sleeping giant. *Emerg. Top.*  
212 *Life Sci.* **1**, 93–103 (2017).

213 11. Rossitto, M., Fiscarelli, E. V. & Rosati, P. Challenges and promises for planning future  
214 clinical research into bacteriophage therapy against *Pseudomonas aeruginosa* in cystic  
215 fibrosis. An argumentative review. *Front. Microbiol.* **9**, 1–16 (2018).

216 12. De Smet, J., Hendrix, H., Blasdel, B. G., Danis-Wlodarczyk, K. & Lavigne, R.  
217 *Pseudomonas* predators: understanding and exploiting phage–host interactions. *Nat.*  
218 *Rev. Microbiol.* **15**, 517–530 (2017).

219 13. Chabas, H., van Houte, S., Høyland-Kroghsbo N. M., Buckling, A. & Westra, E. R.  
220 Immigration of susceptible hosts triggers the evolution of alternative parasite defence  
221 strategies. *Proc. R. Soc. B.* **283** (2016).

222 14. Harrison, F. Microbial ecology of the cystic fibrosis lung. *Microbiology* **153**, 917–923  
223 (2007).

- 224 15. O'Brien, S. & Fothergill, J. L. The role of multispecies social interactions in shaping  
225 *Pseudomonas aeruginosa* pathogenicity in the cystic fibrosis lung. *FEMS Microbiol.*  
226 *Lett.* **364**, 1–10 (2017).
- 227 16. Bhargava, N., Sharma, P. & Capalash, N. Pyocyanin stimulates quorum sensing-  
228 mediated tolerance to oxidative stress and increases persister cell populations in  
229 *Acinetobacter baumannii*. *Infect. Immun.* **82**, 3417–3425 (2014).
- 230 17. Rocha, G. A. *et al.* Species distribution, sequence types and antimicrobial resistance of  
231 *Acinetobacter* spp. from cystic fibrosis patients. *Epidemiol. Infect.* **146**, 524–530 (2018).
- 232 18. Diraviam Dinesh, S. & Diraviam Dinesh, S. Artificial sputum medium. *Protoc. Exch.*  
233 4–7 (2010).
- 234 19. An, D., Danhorn, T., Fuqua, C. & Parsek, M. R. Quorum sensing and motility mediate  
235 interactions between *Pseudomonas aeruginosa* and *Agrobacterium tumefaciens* in  
236 biofilm cocultures. *Proc. Natl. Acad. Sci.* **103**, 3828–3833 (2006).
- 237 20. León, M. & Bastías, R. Virulence reduction in bacteriophage resistant bacteria. *Front.*  
238 *Microbiol.* **6**, 343 (2015).
- 239 21. Kavanagh, K. & Reeves, E. P. Exploiting the potential of insects for *in vivo*  
240 pathogenicity testing of microbial pathogens. *FEMS Microbiol. Rev.* **28**, 101–112  
241 (2004).
- 242 22. Hernandez, R. J. *et al.* Using the wax moth larva *Galleria mellonella* infection model to  
243 detect emerging bacterial pathogens. *PeerJ* **6**, e6150 (2019).
- 244 23. Craig, L., Pique, M. E. & Tainer, J. A. Type IV pilus structure and bacterial  
245 pathogenicity. *Nat. Rev. Microbiol.* **2**, 363–378 (2004).
- 246 24. Johnson, P. T. J., de Roode, J. C. & Fenton, A. Why infectious disease research needs  
247 community ecology. *Science* **349**, 1259504–1259504 (2015).
- 248 25. Alizon, S., de Roode, J. C. & Michalakis, Y. Multiple infections and the evolution of  
249 virulence. *Ecol. Lett.* **16**, 556–567 (2013).
- 250 26. Benmayor, R., Hodgson, D. J., Perron, G. G. & Buckling, A. Host mixing and disease  
251 emergence. *Curr. Biol.* **19**, 764–767 (2009).
- 252 27. Keesing, F. *et al.* Impacts of biodiversity on the emergence and transmission of  
253 infectious diseases. *Nature* **468**, 647–652 (2010).
- 254 28. Chabas, H. *et al.* Evolutionary emergence of infectious diseases in heterogeneous host  
255 populations. *PLOS Biol.* **16**, e2006738 (2018).
- 256 29. van Houte, S. *et al.* The diversity-generating benefits of a prokaryotic adaptive immune  
257 system. *Nature* **532**, 385–388 (2016).



258 30. Wright, R. C. T., Friman, V. P., Smith, M. C. M. & Brockhurst, M. A. Cross-resistance  
259 is modular in bacteria-phage interactions. *PLoS Biol.* **16**, e2006057 (2018).

260

261 **Acknowledgements** The authors thank Prof. A. Buckling for critical reading of the manuscript,  
262 J. Common, E. Hesse and S. Meaden for comments on the manuscript, and Prof. JP Pirnay and  
263 D. de Vos for sharing clinical isolates of *S. aureus*, *A. baumannii*, and *B. cenocepacia*. This  
264 work was supported by grants from the ERC (ERC-STG-2016-714478 - EVOIMMECH) and  
265 the NERC (NE/M018350/1), which were awarded to E.R.W.

266

### 267 **Author Contributions**

268 Conceptualisation of the study was done by E.O.A. and E.R.W. Experimental design was  
269 carried out by E.O.A., A.M.L., C.R. and E.R.W. Adsorption and infection assays were done by  
270 E.O.A. All evolution experiments were performed by E.O.A., E.P. and I.M.. E.O.A. did the  
271 DNA extractions and qPCRs. The competition experiments, virulence assays, and motility  
272 assays were performed by E.O.A. and E.P.. Formal analysis of results was done by E.O.A.,  
273 E.P., C.R. and E.R.W. The original draft was written by E.O.A., with later edits and reviews  
274 done by E.O.A. and E.R.W.

275

### 276 **Author Information**

277 The authors declare no competing interests. Correspondence and requests for materials should  
278 be addressed to E.R.W. (E.R.Westra@exeter.ac.uk) or E.O.A. (eao210@exeter.ac.uk).

279

280 **Figure 1 | Biodiversity affects the evolution of phage resistance.** (a) Proportion of *P.*  
281 *aeruginosa* that acquired surface- (SM) or CRISPR-based resistance, or remained sensitive at  
282 3 d.p.i. with phage DMS3*vir* when grown in monoculture or polycultures, or with an isogenic  
283 surface mutant (6 biologically independent replicates per treatment, and 24 random colonies  
284 phenotypically characterised per replicate). Error bars indicate the mean±one SE. (b) Microbial  
285 community composition over time for the mixed-species infection experiments. Legend  
286 abbreviations: PA14 = *P. aeruginosa*, SA = *S. aureus*, AB = *A. baumannii*, and BC = *B.*  
287 *cenocepacia*.

288

289 **Figure 2 | Biodiversity amplifies fitness costs associated with surface-based resistance.**  
290 Relative fitness of *P. aeruginosa* with CRISPR-based resistance after competing for 24h  
291 against a surface mutant at (a) varying amounts of phage DMS3*vir* in the presence or absence  
292 of a mixed microbial community. Regression slopes with shaded areas corresponding to 95%  
293 CI (n=72). (b) Relative fitness after competition in the absence of phage, but in the presence  
294 of other bacterial species individually or as a mixture. Error bars indicate mean± 95% CI, n=36  
295 for monoculture and polyculture treatments; n=24 for remaining treatments. All sample  
296 numbers represent independent biological replicates.

297

298 **Figure 3 | Evolution of phage resistance affects *in vivo* virulence.** (a) Time-to-death of  
299 *Galleria* (median±one SE) infected with PA14 clones that evolved phage resistance in presence  
300 or absence of the microbial community (n=376; Cox proportional hazards model with Tukey  
301 contrasts). (b) Bacterial motility of clones with CRISPR- or surface-based (SM) phage  
302 resistance (n=981). Boxplots show median, upper and lower 25th and 75th percentiles, inter-  
303 quartile range, and outliers (dots). (c) Time-to-death following infection with PA14 clones with  
304 CRISPR- or surface-based (SM) phage resistance (n=981, presented and analysed as in (a)).  
305 All sample numbers represent independent biological replicates.

306

307 **Methods**

308 All statistical analyses were done using R version 3.5.1. (R Core Team, 2018), and the  
309 Tidyverse package version 1.2.1. (Wickham, 2017). All *Galleria mellonella* mortality analyses  
310 were done using the Survival package version 2.38 (Therneau, 2015).

311

312 **Bacterial strains and viruses.** We used a marked *P. aeruginosa* UCBPP-PA14 mutant  
313 carrying a streptomycin resistant gene inserted into the genome using pBAM1<sup>31</sup> (referred to as  
314 the ancestral PA14 strain). The WT PA14 bacteriophage-insensitive mutant with 2 CRISPR  
315 spacers (BIM2), the surface mutant derived from the PA14 *csy3::LacZ* strain, and phage  
316 DMS3vir and DMS3vir+acrFI (carrying an anti-CRISPR gene) have all been previously  
317 described (refs. 5 and 29 and references therein). The bacteria used as the microbial community  
318 were *Staphylococcus aureus* strain 13 S44 S9, *Acinetobacter baumannii* clinical isolate FZ21  
319 and *Burkholderia cenocepacia* J2315, and were all isolated from patients at Queen Astrid  
320 Military Hospital, Brussels, Belgium.

321

322 **Adsorption and infection assays.** Phage infectivity against each of the bacterial species used  
323 in this study was assessed by spotting serial dilutions of virus DMS3vir on lawns of the  
324 individual community bacteria, followed by checking for any plaque formation after 24 hours  
325 of growth at 37°C. Adsorption assays (as shown in Extended Data Fig. 1) were performed by  
326 monitoring phage titres over time, for up to an hour (At 0, 2, 4, 6, 8, 10, 15 and 20 minutes post  
327 infection for PA14, and at 0, 5, 10, 20, 40 and 60 minutes post infection for the other bacteria  
328 species. For the no-bacterial control, sampling was done at 0 and 60 minutes post infection),  
329 after inoculating the individual bacteria in mid-log phase at approximately  $2 \times 10^8$  c.f.u. with  
330 phage DMS3vir at  $2 \times 10^6$  p.f.u. (final MOI = 0.001). Adsorption assays were carried out in  
331 falcon tubes containing 15ml LB medium, incubated at 37°C while shaking at 180 r.p.m. (three  
332 independent replicates per experiment). At each timepoint, 50µl of sample was transferred to  
333 pre-cooled eppendorfs on ice, containing 900µl LB medium and 50µl chloroform, before  
334 vortexing for 10 seconds. After sampling was completed, all eppendorfs were centrifuged at  
335 full speed at 4 °C for >5 minutes after which 300µl of the supernatant was extracted, diluted  
336 and spotted onto lawns of *P. aeruginosa* before checking for plaque formation after 24h of  
337 growth at 37 °C.

338

339 **Evolution experiments.** The streptomycin resistant mutant of the ancestral strain of *P.*  
340 *aeruginosa* was used for all coevolution experiments. Evolution experiments (shown in Fig. 1,

341 and Extended Data Figs. 2 and 3) were performed by inoculating 60µl from overnight cultures  
342 (containing approximately 10<sup>6</sup> colony-forming units (c.f.u.)) into glass microcosms containing  
343 6ml LB medium (Fig. 1 and Extended Data Fig. 3), or artificial sputum medium<sup>18</sup> (ASM)  
344 (Extended Data Fig. 2). 1 litre of ASM was made by mixing 5g mucin from porcine stomach  
345 (Sigma), 4g low molecular-weight salmon sperm DNA (Sigma), 5.9mg diethylene triamine  
346 pentaacetic acid (DTPA) (Sigma), 5g NaCl (Sigma), 2.2g KCl (Sigma), 1.81g Tris base  
347 (Thermo Fisher Scientific), 5ml egg yolk emulsion (Sigma), and 250mg of each of 20 amino  
348 acids (Sigma), as described in ref. 18. Inoculation was followed by incubation at 37°C while  
349 shaking at 180 r.p.m. (n = 6 per treatment). The polyculture mixes either consisted of  
350 approximately equal amounts of all four bacterial species or mixes of *P. aeruginosa* with just  
351 one additional species where *P. aeruginosa* made up 25% of the total volume used for  
352 inoculation (i.e. 15 µl of 60µl), unless otherwise indicated (i.e. Extended Data Fig. 3). Before  
353 inoculation, phage DMS3vir was added at 10<sup>6</sup> p.f.u. (Fig. 1 and Extended Data Fig. 2), or at  
354 10<sup>4</sup> p.f.u. (Extended Data Fig. 3). Transfers of 1:100 into fresh broth were done daily for a total  
355 of three days. Additionally, phage titres were monitored daily by spotting chlorophorm-treated  
356 lysate dilutions on a lawn of *P. aeruginosa* *csy3::LacZ*. Downstream analysis to determine if  
357 and how bacteria evolved phage resistance was done by cross-streak assays and PCR on 24  
358 randomly selected clones per replicate experiment, as described in ref. 5.

359

360 **DNA extraction and qPCR.** For the experiment shown in Fig. 1, the densities of the different  
361 bacterial species in the microbial communities over time were determined using qPCR. DNA  
362 was extracted from all replicas using the DNeasy UltraClean Microbial Kit (Qiagen), following  
363 the manufacturer instructions. Prior to DNA extraction, to ensure lysis of *S. aureus*, 15µl  
364 lysostaphin (Sigma) at 0.1 mg/ml was added to 500µl of sample followed by incubation at 37°C  
365 for at least one hour. For *P. aeruginosa*, *A. baumannii*, and *B. cenocepacia*, the 16S gene was  
366 chosen as the target for the qPCR primers and were as follows: the PA14 forward primer  
367 (PA14-16s-F), AGTTGGGAGGAAGGGCAGTA; the PA14 reverse primer (PA14-16s-R),  
368 GCTTGCTGAACCACTTACGC; the *A. baumannii* forward primer (AB-16s-F),  
369 ATCAGAATGCCGCGGTGAAT; the *A. baumannii* reverse primer (AB-16s-R),  
370 ACCGCCCTCTTTGCAGTTAG; the *B. cenocepacia* forward primer (BC-16s-F),  
371 ATACAGTCGGGGGATGACGG; the *B. cenocepacia* reverse primer (BC-16s-R),  
372 TCACCAATGCAGTTCCCAGG. For *S. aureus*, we used qPCR primers previously described  
373 in ref. 32. The amplification reactions were performed in triplicates, with Brilliant SYBR Green  
374 reagents (Agilent) in 20µl reactions made up of 10µl master mix, 2µl primer pair, 0.4µl dye,

375 and sterile nuclease free water to a total volume of 15 $\mu$ l before adding 5 $\mu$ l diluted DNA sample.  
376 The qPCR program was as follows: 95°C for 3 minutes, 40 cycles at 95°C for 10 seconds and  
377 60°C for 30 seconds. All qPCR's and results were analysed using the Applied Biosystems  
378 QuantStudio 7 Flex Real-Time PCR system.

379

380 **Competition experiments.** For both competition experiments shown in Fig. 2, the BIM2 clone  
381 was competed against the surface mutant derived from the PA14 *csy3::LacZ* strain<sup>5</sup>. Bacteria  
382 were grown for 24 hours in glass microcosms containing 6ml LB medium, in a shaking  
383 incubator at 180 r.p.m. and at 37°C. For the experiment shown in Fig. 2a, the two phenotypes  
384 were competed in the presence or absence of the mixed microbial community, either without  
385 the addition of phage (n = 36), or infected with phage DMS3vir at 10<sup>4</sup>, 10<sup>6</sup>, and 10<sup>8</sup> p.f.u. (n =  
386 12 per treatment). For the experiment shown in Fig. 2b, the two phage resistant phenotypes  
387 were again competed either in the presence or absence individual bacterial species or a mixed  
388 community of all species. *P. aeruginosa* made up 25% of the total volume of 60 $\mu$ l that was  
389 used to inoculate the 6ml of LB medium (n = 24 per treatment). Samples were taken at 0 and  
390 24 hours post infection., and the cells were serial diluted in M9 salts and plated on cetrimide  
391 agar (Sigma) supplemented with ca. 50 $\mu$ g ml<sup>-1</sup> X-gal (to select for *P. aeruginosa*, while also  
392 differentiating between the CRISPR-resistant clones (white) and the surface mutant (blue)).  
393 Relative fitness was calculated as described in refs. 5 and 29.

394

395 **Virulence assays.** All infection experiments were done using *Galleria mellonella* larvae (UK  
396 WaxWorm Ltd). Throughout the experiments, the larvae were stored in 12-well plates, with  
397 one larva per well, and were all checked for mortality and melanisation before injection.  
398 Bacterial inoculums were prepared depending on experiment, and were as follows; For the  
399 experiment shown in Fig. 3a, all 24 evolved clones from each replicate from the 25%  
400 (community present) and 100% (community absent) treatments (Extended Data Fig. 3) were  
401 pooled together by replica (n = 6 per treatment) and mixed in 6mL of LB medium. Each mixture  
402 of clones was injected into ten individual larvae, with time to death measured as a proxy for  
403 virulence. This procedure was performed in three independent repeats by injecting the same  
404 mixtures of bacterial clones into independent batches of larvae in separate experiments (total  
405 no. of larvae = 420). To assess virulence of all evolved clones (Fig. 3c), infections were done  
406 independently using all the individual PA14 clones from 3 d.p.i. from the experiment shown  
407 in Extended Data Fig. 3 (n = 1008). Here (Fig. 3c), the bacterial inoculums were prepared  
408 individually for each clone by inoculating 200 $\mu$ l LB medium with 5 $\mu$ l bacterial sample from

409 freezer stock, repeated for all individual clones in 96-well plates. Finally, to measure whether  
410 surface-based resistance against an LPS-specific phage was associated with similar virulence  
411 trade-offs (Extended data fig. 7), we isolated *P. aeruginosa* clones from 6 independent  
412 infection experiments with phage LMA2. A total of 10 clones per replicate experiment, isolated  
413 from 3 d.p.i., were phenotypically characterised to confirm resistance, and examined by PCR  
414 to exclude that resistance was CRISPR-based. All 10 clones with LPS-based resistance from  
415 the same replicate experiment were pooled together in 6ml of LB medium (n = 6), and  
416 infections of *G. mellonella* larvae were carried out as described above, with each mixture of  
417 clones injected into ten individual larvae, performed in three independent repeats (total no. of  
418 larvae = 240). Prior to infection, all bacterial inoculums were grown overnight at 37°C on an  
419 orbital shaker (180 r.p.m.) before being diluted by adding 20µl to 180µl of M9 salts. Cell  
420 density was then assayed by measuring OD<sub>600</sub> absorbance, with 0.1OD being ~1 x 10<sup>8</sup> cfu/ml,  
421 before being further diluted down to approximately 10<sup>4</sup> cfu/ml, which was subsequently used  
422 for infection by injecting 10µl into the rear proleg of individual *G. mellonella* using a sterile  
423 syringe as further described in ref. 22. Following infection, larvae were incubated at 28°C, with  
424 mortality monitored hourly for up to 48 hours. For all independent experiments, a control where  
425 larvae were injected with just M9 salts was included. All work conforms to ethical regulations  
426 regarding the use of invertebrates, with approval from The University of Exeter ethics  
427 committee.

428

#### 429 **Motility assays.**

430 Swarming motility of all evolved bacterial clones from the experiment shown in Extended Data  
431 Fig. 3c (n = 1008) was assayed by using a 96-well microplate pin replicator to stamp the  
432 individual clones on 1% agar before overnight growth at 37°C. The diameters of the individual  
433 clones were then taken as a measure of motility (three replicas per clone).

434

#### 435 **Data Availability Statement**

436 All data used in this study is available on figshare at [10.6084/m9.figshare.9752903](https://figshare.com/10.6084/m9.figshare.9752903).

437

#### 438 **Methods references**

- 439 31. Martínez-García, E., Calles, B., Arévalo-Rodríguez, M. & de Lorenzo, V. pBAM1: an  
440 all-synthetic genetic tool for analysis and construction of complex bacterial phenotypes.  
441 *BMC Microbiol.* **11**, 38 (2011).
- 442 32. Goto, M. *et al.* Real-time PCR method for quantification of *Staphylococcus aureus* in

443 milk. *J. Food. Prot.* **70**, 90-96 (2006).

444

445 **Extended Data Figure 1. Only *P. aeruginosa* adsorbs phage DMS3vir.** Phage levels, given  
446 in plaque-forming units per millilitre, over time in minutes post infection of *P. aeruginosa*  
447 PA14 and three other bacterial species (n = 252 biologically independent samples). Controls  
448 were carried out in the absence of bacteria. Lines are regression slopes with shaded areas  
449 corresponding to 95% confidence intervals. Linear model: Effect of *P. aeruginosa* on phage  
450 titre over time; t = -3.37, p = 0.0009; *S. aureus*; t = 1.63, p = 0.11; *A. baumannii*; t = 1.20, p =  
451 0.23; *B. cenocepacia*; t = -0.27, p = 0.79; Overall model fit;  $F_{9,235} = 4.33$ , adjusted  $R^2 = 0.11$ , p  
452 =  $3.17 \times 10^{-5}$ .

453

454 **Extended Data Figure 2. Enhanced CRISPR resistance evolution in artificial sputum**  
455 **medium.** Proportion of *P. aeruginosa* that acquired surface modification (SM) or CRISPR-  
456 based immunity (or remained sensitive) at 3 days post infection with phage DMS3vir when  
457 grown in artificial sputum medium (6 biologically independent replicates per treatment, and 24  
458 random colonies phenotypically characterised per replicate). Deviance test: Relationship  
459 between community composition and CRISPR; Residual deviance(25, n = 30) = 1.26, p =  $2.2$   
460  $\times 10^{-16}$ ; Tukey contrasts: Monoculture v Mixed; z = -5.30, p =  $1 \times 10^{-4}$ ; Monoculture v *A.*  
461 *baumannii*; z = -5.60, p =  $1 \times 10^{-4}$ ; Monoculture v *B. cenocepacia*; z = -2.80, p = 0.02;  
462 Monoculture v *S. aureus*; z = -0.76, p = 0.93. Error bars correspond to  $\pm$  one standard error,  
463 with the mean as the measure of centre.

464

465 **Extended Data Figure 3. Increased CRISPR-based resistance evolution across a range of**  
466 **microbial community compositions over time.** Proportion of *P. aeruginosa* that acquired  
467 surface modification (SM) or CRISPR-based immunity (or remained sensitive) at up to 3 days  
468 post infection (d.p.i.) with phage DMS3vir when grown either in monoculture (100%), or in  
469 polyculture mixtures consisting of the mixed microbial community but with varying starting  
470 percentages of *P. aeruginosa* based on volume (3-6 biologically independent replicates per  
471 treatment as indicated in the figures, and 24 random colonies phenotypically characterised per  
472 replicate). **(a)** Resistance evolution at 1 d.p.i. Error bars correspond to  $\pm$  one standard error,  
473 with the mean as the measure of centre. Deviance test: Relationship between CRISPR and *P.*  
474 *aeruginosa* starting percentage at timepoint 1; Residual deviance(34, n = 41) = 4.42, p = 0.004;  
475 1%; z = -3.27, p = 0.002; 10%; z = 1.21, p = 0.23; 25%; z = 1.62, p = 0.11; 50%; z = 2.20, p =  
476 0.034; 90%; z = 2.07, p = 0.046; 99%; z = 0.47, p = 0.65; 100%; z = 1.47, p = 0.15. **(b)**  
477 Resistance evolution at 2 d.p.i. Error bars correspond to  $\pm$  one standard error, with the mean as  
478 the measure of centre. Deviance test: Relationship between CRISPR and *P. aeruginosa* starting



479 percentage at timepoint 2; Residual deviance(25, n = 32) = 3.86,  $p = 2.51 \times 10^{-6}$ ; 1%;  $z = -2.14$ ,  
480  $p = 0.04$ ; 10%;  $z = 1.19$ ,  $p = 0.25$ ; 25%;  $z = 2.07$ ,  $p = 0.049$ ; 50%;  $z = 1.89$ ,  $p = 0.07$ ; 90%;  $z =$   
481  $1.12$ ,  $p = 0.27$ ; 99%;  $z = 1.21$ ,  $p = 0.24$ ; 100%;  $z = 1.11$ ,  $p = 0.28$ . (c) Resistance evolution at  
482 3 d.p.i. Error bars correspond to  $\pm$  one standard error, with the mean as the measure of centre.  
483 Deviance test: Relationship between CRISPR and *P. aeruginosa* starting percentage at  
484 Timepoint 3; Residual deviance(35, n = 42) = 8.24,  $p = 0.0004$ ; 1%;  $z = -3.38$ ,  $p = 0.002$ ; 10%;  
485  $z = 2.12$ ,  $p = 0.04$ ; 25%;  $z = 2.77$ ,  $p = 0.009$ ; 50%;  $z = 3.07$ ,  $p = 0.004$ ; 90%;  $z = 2.46$ ,  $p =$   
486  $0.019$ ; 99%;  $z = 1.55$ ,  $p = 0.13$ ; 100%;  $z = 0.87$ ,  $p = 0.39$ .

487

488 **Extended Data Figure 4. Microbial community composition impacts phage epidemic size.**

489 The DMS3vir phage titres (in plaque-forming units per millilitre) over time up to 3 days post  
490 infection of *P. aeruginosa* grown either in monoculture (100%), or in polyculture mixtures as  
491 shown in Extended Data Fig. 3. Each data point represents the mean, with error bars  
492 corresponding to  $\pm$  one standard error (n=6 independent biological replicates per treatment).  
493 Two-way ANOVA: Overall effect of *P. aeruginosa* starting percentage on phage titre;  $F_{6,105} =$   
494  $14.84$ ,  $p = 1.1 \times 10^{-12}$ .

495

496 **Extended Data Figure 5. No correlation between phage epidemic size and evolution of**

497 **CRISPR resistance.** The correlation between the proportion of evolved CRISPR-based  
498 resistance at 3 d.p.i. and the phage epidemic sizes (in plaque-forming units per millilitre) in the  
499 presence of other bacterial species, using data taken from experiments shown in Fig. 1,  
500 Extended Data Fig. 2, Extended Data Fig. 3c and Extended Data Fig. 6 (n = 137 biologically  
501 independent samples per timepoint). Correlations are separated by day, as phage titres were  
502 measured daily. The lines indicate regression slopes, with shaded areas corresponding to 95%  
503 confidence intervals. Pearson's Product-Moment Correlation tests between phage titres (at  
504 each day post infection) and levels of CRISPR-based resistance: T = 1;  $t_{136} = -0.02$ ,  $p = 0.98$ ,  
505  $R^2 = -0.002$ ; T = 2;  $t_{136} = 0.59$ ,  $p = 0.55$ ,  $R^2 = 0.05$ ; T = 3;  $t_{136} = -0.90$ ,  $p = 0.37$ ,  $R^2 = -0.08$ .

506

507 **Extended Data Figure 6. Starting phage titre does not affect CRISPR evolution in the**  
508 **presence of a microbial community.** Proportion of *P. aeruginosa* that acquired CRISPR-

509 based resistance at 3 days post infection with varying starting titres of phage DMS3vir when  
510 grown in polyculture (n = 6 biologically independent replicates per treatment, and 24 random  
511 colonies phenotypically characterised per replicate). Deviance test: Start phage and CRISPR;  
512 Residual deviance(20, n = 24) = 2.00,  $p = 0.13$ ; Tukey contrasts:  $10^2$  v  $10^4$ ;  $z = -1.52$ ,  $p = 0.42$ ;

513  $10^4$  v  $10^6$ ;  $z = -0.76$ ,  $p = 0.87$ ;  $10^6$  v  $10^8$ ;  $z = 1.31$ ,  $p = 0.56$ ;  $10^2$  v  $10^6$ ;  $z = -2.24$ ,  $p = 0.11$ ;  $10^2$   
514 v  $10^8$ ;  $z = -0.99$ ,  $p = 0.75$ ;  $10^4$  v  $10^8$ ;  $z = 0.56$ ,  $p = 0.94$ . Error bars correspond to  $\pm$  one standard  
515 error, with the mean as the measure of centre.

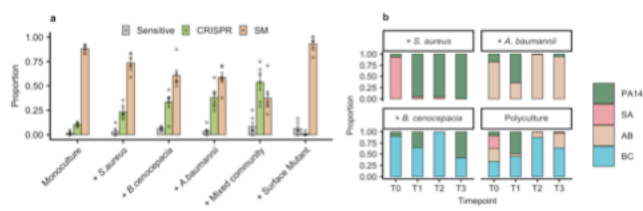
516

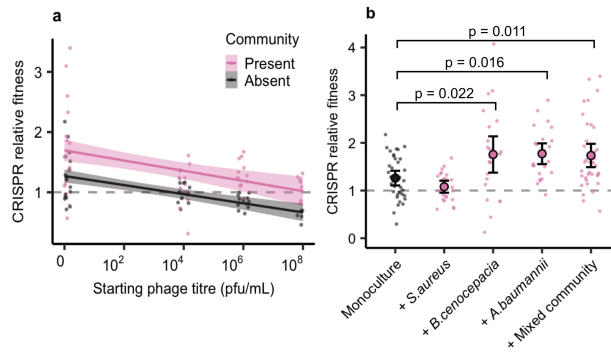
517 **Extended Data Figure 7. LPS-based phage resistance also affects in vivo virulence.** Time  
518 to death (given as the median  $\pm$  one standard error) for *Galleria mellonella* larvae infected with  
519 PA14 clones that evolved phage resistance against phage LMA2, which is assumed to occur  
520 through LPS modification, compared to the phage-sensitive ancestral ( $n = 209$  biologically  
521 independent samples). Cox proportional hazards model with Tukey contrasts: Sensitive  
522 (ancestral) v LPS ;  $z = 4.81$ ,  $p = 1.49 \times 10^{-6}$ . Overall model fit;  $LRT_3 = 44.94$ ,  $p = 1 \times 10^{-9}$ .

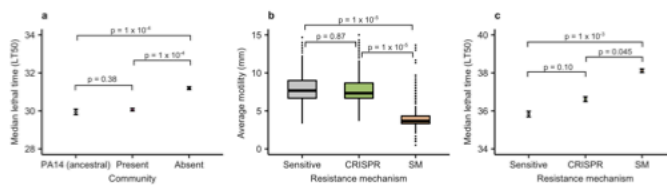
523

524

525







533

534

535

